SPEKTRA: Jurnal Fisika dan Aplikasinya
Volume 11, Issue 1, April 2026
Homepage: doi.org/10.21009/SPEKTRA

DOI: doi.org/10.21009/SPEKTRA.111.04

Shakemap and Focal Mechanism Analysis of the December 2024 Gresik Earthquake

Mochamad Tanwiruz Zaman[1,2], Agus Suprianto[1], Lutfi Rohman[1,*], Bowo Eko Cahyono[1]

[1]*Physics Department, University of Jember, Jl. Kalimantan 37 Jember - Indonesia*
[2]*BMKG Pasuruan, Jl. Sedap Malam, Pandaan, Pasuruan, Indonesia*

*Corresponding Author Email: el_rahman.fmipa@unej.ac.id

Received: 26 January 2026
Revised: 8 April 2026
Accepted: 30 April 2026
Online: 30 April 2026
Published: 30 April 2026

SPEKTRA: Jurnal Fisika dan Aplikasinya
p-ISSN: 2541-3384
e-ISSN: 2541-3392

ABSTRACT

An earthquake that occurred on December 30, 2024 in Gresik Regency, located at 7.05° S and 112.62° E with a focal depth of 14 km and magnitude M3.3, was a shallow earthquake felt with an intensity of II–III MMI. This study aims to analyze the earthquake shaking intensity map (Shakemap), determine the earthquake source mechanism, and perform earthquake scenario modeling using the maximum magnitude based on the Indonesian Earthquake Source and Hazard Map (PUSGEN). Shakemap analysis was carried out using the BMKG Shakemap server based on accelerograph network data. Fault mechanism analysis was performed using focal mechanism software with P-wave polarity input obtained from waveform signal picking using SeisGram2K software. Meanwhile, the Shakemap scenario was generated using the ShakeMap application available at the Pasuruan Geophysical Station. The results show that the distribution of Peak Ground Acceleration (PGA) and shaking intensity is influenced not only by the distance from the epicenter but also by local geological conditions that contribute to ground-motion amplification. Source mechanism analysis indicates that the Gresik earthquake was dominated by a strike-slip faulting mechanism with a weak oblique component, interpreted as sinistral strike-slip motion along the RMKS–Tuban 3 fault zone. Scenario earthquake modeling with a magnitude of M 6.2 indicates that Gresik Regency has the potential to experience strong ground shaking with maximum intensities reaching VI–VII MMI, while surrounding areas such as Surabaya City, eastern Lamongan Regency, and western Bangkalan Regency may experience intensities up to VI MMI. These findings indicate that although the Gresik earthquake had a relatively small magnitude, the potential earthquake impact in Gresik and surrounding areas could become significant if a maximum-magnitude earthquake occurs,

therefore, this study provides important information for earthquake disaster mitigation efforts.

Keywords: earthquake hazard, shakemap, focal mechanism, ground motion, peak ground acceleration

INTRODUCTION

Indonesia is located at the convergence of three major tectonic plates, namely the Eurasian Plate, the Indo-Australian Plate, and the Pacific Plate. The movement and interaction of these plates make Indonesia a region with complex tectonic conditions and high geological activity, resulting in frequent occurrences of earthquakes, tsunamis, volcanic eruptions, and other natural hazards [1-2]. An earthquake is a ground vibration caused by the sudden release of energy within the Earth's crust as a result of tectonic plate movements. These plate movements occur along convergent (collisional), divergent (spreading), and transform (sliding) plate boundaries, as well as along active fault zones on land, when rocks are no longer able to withstand stresses exceeding their elastic limits. The released energy propagates in all directions in the form of seismic waves, allowing earthquake shaking to be felt at the Earth's surface [3-5].

In East Java Province, several active faults, including the Kendeng Fault, RMKS Fault, Pasuruan Fault, Probolinggo Fault, and Wongsorejo Fault, exhibit significant seismic potential and play an important role in generating local earthquakes that may affect densely populated areas [6]. Gresik Regency and its surrounding areas are located within an active tectonic deformation zone influenced by more than one fault system, namely the Kendeng Fault Zone and the RMKS (Rembang–Madura–Kangean–Sakala) Fault system. The Kendeng Fault Zone extends across northern East Java and acts as one of the primary sources of shallow earthquakes in the region. The RMKS Fault Zone is a left-lateral strike-slip fault system trending west–east, extending from Rembang to the offshore Sakala area, with an approximate length of 675 km and a deformation width of 15–40 km [7]. The interaction and tectonic activity of these two fault systems are believed to contribute to the occurrence of local earthquakes in Gresik, Surabaya, and surrounding areas. Therefore, analyzing earthquake source mechanisms is essential for understanding regional seismic characteristics and potential seismic hazards. Historical seismicity records indicate that Gresik Regency has experienced earthquakes with significant impacts in the past. According to the BMKG Earthquake Catalog, an earthquake on 31 August 1902 produced shaking intensities reaching VI MMI in the Gresik area. Furthermore, on 19 June 1950, an earthquake with even higher intensity, reaching VII MMI, was recorded, indicating that this region has a history of damaging earthquakes [8]. These historical records suggest that the potential for strong ground shaking in Gresik is not a new phenomenon and requires serious consideration in disaster risk assessments.

On 30 December 2024 at 12:38:40 WIB, another earthquake with a magnitude of 3.3 and a hypocentral depth of approximately 14 km occurred in Manyar District, Gresik Regency. The epicenter was located relatively close to the Java Integrated Industrial and Ports Estate (JIIPE), one of Indonesia's strategic industrial and infrastructure zones. The earthquake epicenter

located in Manyar District, Gresik Regency, is situated in a geological setting characterized by alluvial deposits dominated by clay. These alluvial deposits were formed during the Holocene and are directly bordered by the Madura Strait. Sedimentary deposits along the Madura Strait were formed by coastal deposits extending inland up to approximately ±5 km. The coastal deposits consist of silty clay and clayey silt, with thin intercalations that generally contain abundant shell fragments in several locations [9]. Although the earthquake was small in magnitude and did not cause significant damage, the shaking was clearly felt by local residents. According to BMKG reports, the shaking intensity reached II–III MMI in Manyar District and parts of Gresik Regency.

The proximity of the epicenter to a strategic industrial area, combined with the historical record of damaging earthquakes, indicates that even small-magnitude earthquakes may have important implications for earthquake risk assessment in this region. Therefore, analyzing earthquake source mechanisms and conducting ShakeMap modeling are crucial for describing the spatial distribution of shaking intensity. ShakeMap modeling provides quantitative information on affected areas and supports disaster mitigation efforts through the identification of regions potentially susceptible to damage. Although previous studies on regional tectonics and seismic activity in East Java exist, detailed analyses integrating ShakeMap observations, focal mechanism interpretation, and scenario-based modeling for local earthquakes in the Gresik area remain limited. Most earlier studies have focused on regional tectonics or large-magnitude earthquake events, whereas smaller but felt earthquakes occurring near critical infrastructure areas have not yet been comprehensively analyzed. Therefore, this study aims to fill this gap by integrating ShakeMap observation data, focal mechanism analysis, and scenario-based modeling to achieve a better understanding of local seismic hazards in Gresik Regency and the surrounding areas, thereby contributing scientifically to earthquake disaster risk reduction efforts in Gresik Regency and its vicinity.

METHODS

Shakemap Processing (Ground Shaking Intensity Map)

Shakemap (ground shaking intensity map) is a map that illustrates the spatial distribution of earthquake ground shaking at the Earth's surface, expressed in terms of ground acceleration (gal) as well as earthquake intensity using the Modified Mercalli Intensity (MMI) scale [10-11]. This map provides rapid information on the potential impacts of an earthquake on infrastructure and communities. The data used in this study consist of ground acceleration records from the BMKG accelerograph network that recorded the Gresik earthquake on December 30, 2024. The stations used include GRJI (Gresik), MLJM (Lamongan), BLJI (Banyuglugur), PCJI (Pacitan), and KWJI (Wonosobo). ShakeMap processing was carried out using a spatial interpolation approach based on a combination of the Ground Motion Prediction Equation (GMPE) model and observational data from accelerograph stations. The ground acceleration value at a given point was calculated using a weighting method based on the variance of each data source [10]. The ground acceleration value at a point (x^*, y^*) is modeled by EQUATION (1), expressed as:

$$\overline{Y_{xy}} = \frac{\frac{Y_{GMPE,xy}}{\sigma^2_{GMPE}} + \sum_{i=1}^{n} \frac{Y_{obs,xy,i}}{\sigma^2_{obs,xy,i}} + \sum_{j=1}^{n} \frac{Y_{conv,xy,j}}{\sigma^2_{conv,xy,j}}}{\frac{1}{\sigma^2_{GMPE}} + \sum_{i=1}^{n} \frac{1}{\sigma^2_{obs,xy,i}} + \sum_{j=1}^{n} \frac{1}{\sigma^2_{conv,xy,j}}}, \quad (1)$$

where $Y_{GMPE,xy}$ and σ^2_{GMPE} are the amplitude and its variance at the point (x^*, y^*) obtained from the GMPE model; $Y_{obs,xy,i}$ and $\sigma^2_{obs,xy,i}$ are the observed amplitudes and its variance associated with observation i at the point (x^*, y^*); $Y_{conv,xy,j}$ and $\sigma^2_{conv,xy,j}$ are the converted amplitudes and its variance associated with converted observation j at the point (x^*, y^*).

Where the parameters Y_{GMPE}, Y_{obs}, and Y_{conv} respectively represent the acceleration values derived from the GMPE model, observational data, and conversion results, with weights determined by the variance of each parameter. This approach enables the integration of empirical models and observational data to produce a more representative ground-shaking distribution. Furthermore, the obtained ground acceleration (PGA) values were converted into the MMI intensity scale using an empirical relationship [12], as presented in TABLE 1. This

TABLE 1. Shakemap intensity scale.

INSTR. INTENSITY	PERCEIVED SHAKING	PGA (%g)	PGV (cm/s)	DESCRIPTION
I	Not felt	< 0.05	< 0.02	Not felt except by very few under especially favorable conditions
II	Weak	0.3	0.1	Felt only by a few persons at rest, especially on upper floors of buildings. Delicately suspended objects may swing
III	Weak	0.3	0.1	Felt quite noticeably by persons indoors, especially on upper floors c buildings. Many people do not recognize it as an earthquake. Standing motor cars may rock slightly. Vibration similar to the passing of a truck. Duration may be estimated
IV	Light	2.8	1.4	Felt indoors by many, outdoors by few during the day. At night, som awakened. Dishes, windows, doors disturbed; walls make cracking sound. Sensation like heavy truck striking building. Standing motor cars rocked noticeably
V	Moderate	6.2	4.7	Felt by nearly everyone; many awakened. Some dishes, windows broken. Unstable objects overturned. Pendulum clocks may stop
VI	Strong	12	9.6	Felt by all. People alarmed. Some run outside. Light sleepers wakened. Dishes, windows broken. Some furniture moved or overturned. Weak plaster walls cracked.
VII	Very Strong	22	20	Difficult to stand. Noticed by motorcar drivers. Hanging objects quiver. Furniture breaks. Damage to masonry D, including cracks. Weak chimneys broken at roofline. Fall of plaster, loose bricks, stones, tiles
VIII	Severe	30	41	Damage to masonry C and partial collapse. Some damage to masonr B; none to masonry A. Fall of stucco and some masonry walls. Twisting, fall of chimneys, factory stacks, monuments, towers. Fram houses move on foundations if not bolted down
IX	Violent	75	86	General panic. Masonry D destroyed; masonry C heavily damaged, sometimes collapsing. Masonry B seriously damaged. General damage to foundations. Frame structures, if not bolted, shift off foundations.
X	Extreme	>179	>178	Most masonry and frame structures destroyed with foundations. Som well-built wooden structures destroyed. Serious damage to dams, dikes. Large landslides. Water thrown on banks of canals, rivers, lakes.

conversion aims to interpret the level of ground shaking in a form that is easier to understand in the context of its impact on humans and buildings.

The results of the ShakeMap processing, in the form of PGA distribution maps and MMI intensity maps, were then analyzed to identify variations in the level of ground shaking in each area. In addition, the relationship between PGA values and distance from the epicenter was analyzed by constructing a graph of PGA variation based on the distance of accelerograph stations.

Uncertainty in ShakeMap analysis may be influenced by limitations in the number and distribution of accelerograph stations, the quality of recorded data, as well as the role of Ground Motion Prediction Equations (GMPE) used to estimate ground motion in areas with sparse or no observations. These factors may affect the interpolation results and the estimated distribution of ground shaking within the study area [10, 13-14].

Fault Identification Using P-Wave Polarity

The determination of the earthquake focal mechanism was carried out using three-component waveform data to obtain the nodal plane parameters (strike, dip, and rake), which were used to identify the type of active fault (Khoiridah et al., 2023). The earthquake focal mechanism is represented in the form of a focal sphere diagram (beachball diagram), which illustrates the seismic wave radiation pattern and the geometry of the fault plane based on the distribution of compressional and dilatational motions [15]. In this stage of data processing, three types of data were used: earthquake parameter data, waveform data, and station metadata, all of which were obtained from BMKG. Data selection was carried out based on good signal quality and clear P-wave phase identification to ensure accuracy in the analysis process. The initial step in determining the earthquake source mechanism involved identifying the first-motion polarity of the P-wave, namely upward motion (compression) and downward motion (dilatation), using the Seisgram2K software. SeisGram2K merupakan perangkat lunak berbasis Java yang digunakan untuk analisis interaktif data seismik, termasuk picking fase P dan S, filtering sinyal, serta analisis komponen gelombang [16]. The identified polarities were then converted into numerical values, where compression was assigned a value of 1 and dilatation a value of −1. The converted data, including P-wave polarity, latitude, longitude, hypocenter depth, and the coordinates of the earthquake recording stations, were then processed using the Azmtak software to obtain the station azimuth and take-off angle parameters. The output parameters from the Azmtak software were subsequently processed using the PINV software to classify the data based on take-off angle and azimuth, allowing the compression and dilatation zones to be distinguished and subsequently projected in the form of a focal sphere. Based on the results obtained from the PINV analysis, fault parameters were derived and used to identify the focal mechanism of the earthquake source [17-18]. The final fault model of the earthquake source was determined based on the strike, dip, and rake parameters obtained from the focal mechanism analysis. The results produced two nodal planes representing possible fault planes. The selection of the fault plane interpreted as the principal fault plane was carried out by considering the consistency of the nodal plane orientation with the regional geological setting,

in this case the RMKS–Tuban 3 fault system, which trends approximately west–east. In addition, the rake value was used to identify the type of fault movement, so that the selected nodal plane was not only consistent in orientation but also compatible with the fault movement mechanism developed in the study area.

Shakemap Scenario Modeling Processing

The Shakemap scenario modeling applied in this study follows the methodology operationally used by the Indonesian Agency for Meteorology, Climatology, and Geophysics (BMKG), This approach is consistent with the deterministic seismic hazard analysis (DSHA) method, which is used to estimate the maximum ground acceleration based on a specific earthquake source scenario [19]. The ShakeMap system is used to map the spatial distribution of earthquake ground shaking in terms of physical ground-motion parameters and macroseismic intensity, both for actual earthquake events and for scenario-based simulations. The initial stage in generating a ShakeMap involves defining the earthquake source parameters, including magnitude, epicentral and hypocentral locations, and source mechanism. The determination of earthquake scenario parameters generally refers to the maximum magnitude of active faults based on the national earthquake source and hazard map, while also considering the epicenter location and hypocenter depth to represent the worst-case condition [20]. Once the source parameters are defined, strong ground motion at bedrock is calculated using a Ground Motion Prediction Equation (GMPE). GMPEs are empirical relationships derived from statistical regression of earthquake strong-motion records, which are used to predict ground-motion parameters such as Peak Ground Acceleration (PGA) and Peak Ground Velocity (PGV) as functions of earthquake magnitude, source-to-site distance, and hypocentral depth. In general, the GMPE formulation can be conceptually expressed by EQUATION (2) as:

$$\ln(Y) = f(M, R, h, S) + \varepsilon, \tag{2}$$

where Y represents the ground-motion parameter, M is the earthquake magnitude, R is the distance to the seismic source, h is the hypocentral depth, S denotes site conditions, and ε represents the residual term accounting for model uncertainty [21].

The selection of GMPEs in the BMKG ShakeMap system is adjusted to the tectonic environment of the earthquake source, such as shallow crustal faults, subduction interface events, or intraslab earthquakes, as well as the magnitude and depth ranges of the earthquake. Ground-motion values initially calculated at bedrock are subsequently corrected by considering local site effects, since local geological conditions, particularly sedimentary layers, can significantly amplify earthquake ground shaking. In the operational implementation of ShakeMap by BMKG, local site effects are represented by the average shear-wave velocity in the upper 30 meters (Vs30). When direct Vs30 measurements are not available, Vs30 values are estimated using a topographic slope approach derived from Digital Elevation Model (DEM) data. Site amplification corrections are applied linearly based on site class, without considering nonlinear soil behavior, so that the resulting Shakemap reflects a practical and operational approach for regional ground-shaking mapping. After PGA and PGV values are obtained at each grid point, these parameters are converted into macroseismic

intensity, such as Modified Mercalli Intensity (MMI), using empirical relationships between ground motion and intensity. Intensity maps are presented because they are more easily understood by the public and stakeholders compared to purely physical ground-motion parameters. All calculation steps, spatial interpolation, and map visualization are performed using the ShakeMap software. In scenario ShakeMap modeling, the computation is entirely based on source parameters, selected GMPEs, and local site-effect corrections, without incorporating field observation data, so that the resulting Shakemap represents a theoretical distribution of ground shaking [22].

In this study, the modeling was carried out using the BMKG ShakeMap application by inputting the parameters of the 30 December 2024 Gresik earthquake, including the origin time, epicenter location, depth, and maximum magnitude based on PUSGEN (2024). The resulting output consisted of PGA distribution maps and MMI intensity maps, which were then used to analyze the potential earthquake impact in Gresik Regency and the surrounding areas. Uncertainty in this scenario modeling may be influenced by the selection of the GMPE, the estimation of topography-based Vs30 parameters, as well as the assumption that the earthquake source conditions and wave propagation medium are homogeneous. Therefore, the obtained results represent a theoretical scenario that may differ from the actual field conditions. The research flowchart is shown in FIGURE 1.

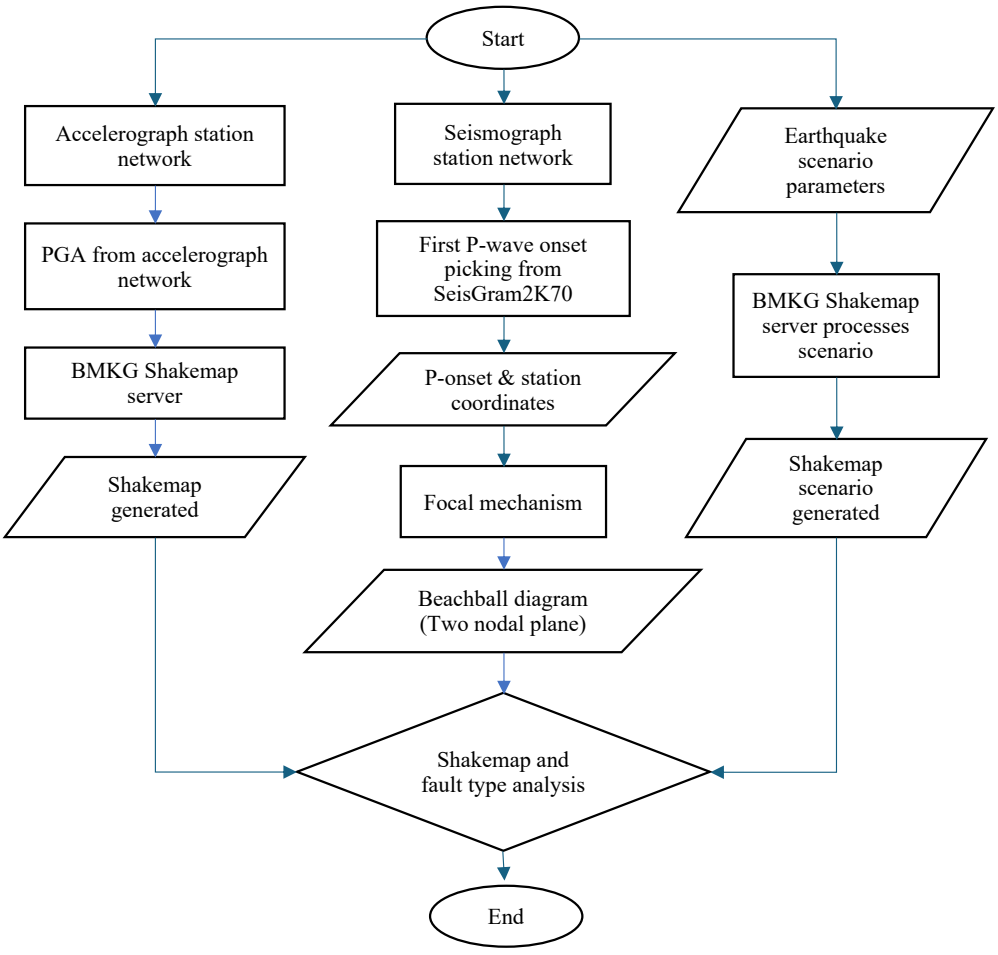

FIGURE 1. The research flowchart.

TABLE 2. PGA, MMI, and Distance of BMKG Accelerograph Stations for the Gresik Earthquake

No	ID Station	Station	Lat	Lon	Distance	PGA-EW(gal)	PGA-NS(gal)	PGA-UD(gal)
1	GRJI	Gresik, East Java	-6.915	112.479	21.66	0.1156	0.0970	0.0892
2	MLJM	Mantup, Lamongan, East Java	-7.248	112.338	38.13	0.6644	0.5243	0.2597
3	BLJI	Banyuglugur, East Java	-7.745	113.595	132.41	0.0480	0.0196	0.0206
4	PCJI	Pacitan, East Java	-8.195	111.177	203.70	0.0078	0.0059	0.0039
5	KWJI	Wonosobo, Central Java	-7.384	109.969	294.79	0.1392	0.1460	0.3508

RESULTS AND DISCUSSION

Shakemap Processing (Ground Shaking Intensity Map)

The Shakemap was generated using input data from accelerograph stations that recorded the earthquake ground motion. Ground acceleration values recorded at each station were modeled to produce a ground shaking intensity map. The earthquake that occurred in Gresik on December 30, 2024 was recorded by several BMKG accelerograph stations and was felt by the population in Gresik and surrounding areas. The accelerograph stations that recorded this event include GRJI (Gresik), MLJM (Lamongan), BLJI (Banyuglugur), PCJI (Pacitan), and KWJI (Wonosobo). The Peak Ground Acceleration (PGA) values recorded at each station are presented in TABLE 2.

The highest peak ground acceleration (PGA) recorded during the Gresik earthquake was observed at the MLJM Lamongan station, with values of 0.6644 gal (EW component), 0.5243 gal (NS component), and 0.2597 gal (UD component). This station is not the closest to the epicenter, with a distance of 38.13 km. The higher PGA value observed at station MLJM compared to station GRJI, which is located closer to the epicenter, indicates that distance is not the only controlling factor of ground-shaking amplitude. This difference is presumed to be influenced by local geological conditions (site effect), where station MLJM is likely situated on softer sediment layers that are capable of amplifying seismic waves. Soft soil conditions generally have low shear-wave velocity (Vs30), thereby causing an increase in vibration amplitude compared to areas composed of more compact rock [23]. In addition to soil conditions, differences in PGA values may also be influenced by wave propagation paths (path effect) as well as subsurface structural heterogeneity. The relatively high vertical PGA value (UD component) at station KWJI compared to other stations, despite being located farthest from the epicenter, indicates the presence of a data anomaly (outlier). This condition may be caused by several factors, such as possible instrumental noise, the effect of a deep sedimentary basin, or the influence of non-homogeneous seismic wave propagation paths. Therefore, this value needs to be interpreted carefully and should not be directly considered representative of the general regional condition. The results of the Shakemap modeling are illustrated in FIGURE 2.

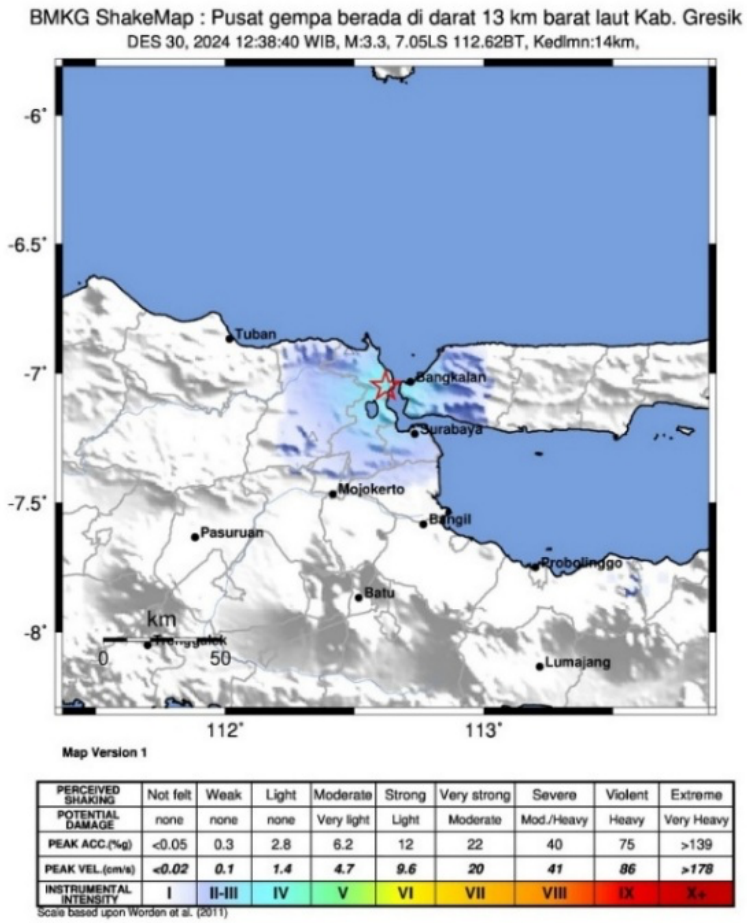

FIGURE 2. Shakemap of the Gresik earthquake on December 30, 2024.

Based on FIGURE 2, it can be observed that the maximum earthquake intensity (MMI) of the 30 December 2024 Gresik earthquake with a magnitude of 3.3 reached Intensity III MMI, which is characterized by vibrations clearly felt indoors, resembling the sensation of a passing truck. This intensity distribution indicates that the earthquake was shallow and was significantly felt by communities around the epicenter. Intensity III MMI was felt in Manyar, Bungah, and Sedayu Districts (Gresik Regency), as well as in Socah District (Bangkalan Regency). Meanwhile, Intensity II MMI was felt in Lamongan Regency, including Kalitengah District, Lamongan City, Tikung District, Karangbinangun District, Deket District, and Sarirejo District. In addition, Intensity II MMI was also felt in several districts in southern Gresik Regency, including Balongpanggang, Benjeng, Duduk Sampeyan, and surrounding areas. This relatively limited intensity distribution is consistent with the small earthquake magnitude (M 3.3), yet it still indicates that local geological conditions may influence the spatial distribution of perceived ground shaking. The variation of Peak Ground Acceleration (PGA) values with respect to the distance of accelerograph stations for the 30 December 2024 Gresik earthquake is shown in the graph in FIGURE 3.

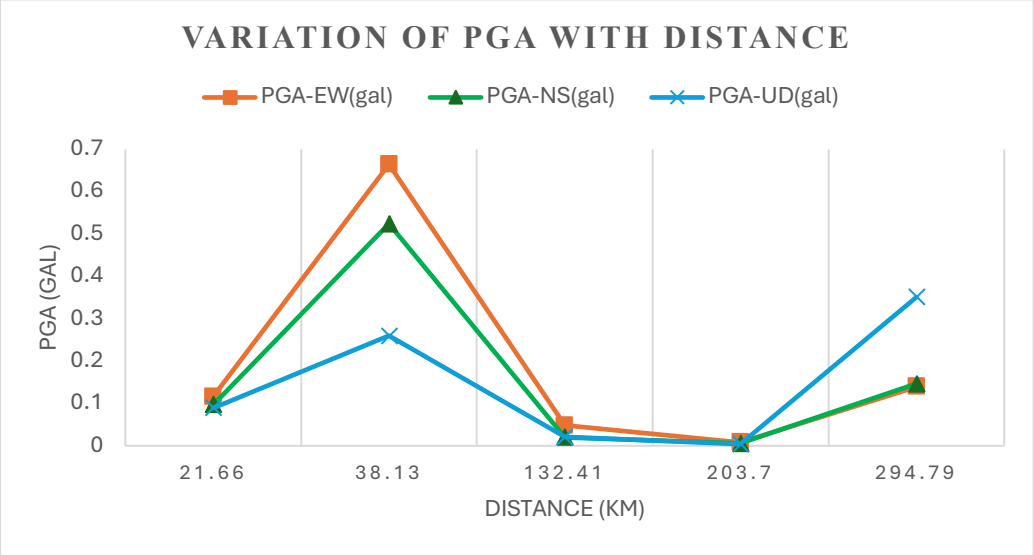

FIGURE 3. Graph of variation of PGA value based on accelerograph station distance.

In general, the variation of PGA demonstrates a strong relationship with epicentral distance. Accelerograph recordings from several stations indicate that PGA values tend to decrease as the distance from the earthquake source increases. This pattern indicates the presence of seismic wave attenuation, in which earthquake energy decreases as a result of propagation through the Earth's medium as well as the influence of wave propagation geometry [24]. However, deviations from this pattern, such as those observed at stations MLJM and KWJI, indicate the influence of factors other than distance, such as local geological conditions and seismic wave propagation paths. However, in addition to distance, PGA values are also strongly influenced by local site effects, geological conditions, and the direction of seismic wave propagation. Variations in lithology, sediment thickness, and subsurface structure can amplify or attenuate seismic wave amplitudes, resulting in differences in ground motion intensity even at locations farther from the earthquake source [14, 23]

Fault Type Analysis Based on the Focal Mechanism Model

The initial step in determining the earthquake source mechanism was conducted by identifying the first-motion polarity of the P-wave, namely upward motion (compression) and downward motion (dilatation), using the Seisgram2K software, as shown in FIGURE 4. The P-wave polarity identification method is a classical approach in focal mechanism analysis used to determine the orientation of the fault plane based on the distribution of compressional and dilatational motions on the focal sphere. This approach is widely used in seismological studies because it is capable of providing preliminary information on earthquake source characteristics, including fault type and the orientation of the principal stress axes [25, 26]

The determination of P-wave polarity was performed through a picking process on the earthquake waveform data obtained from the BMKG seismograph network. The identified polarities were then converted into numerical values, where compression was assigned a value of 1 and dilatation a value of −1, and subsequently used as input for focal mechanism analysis.

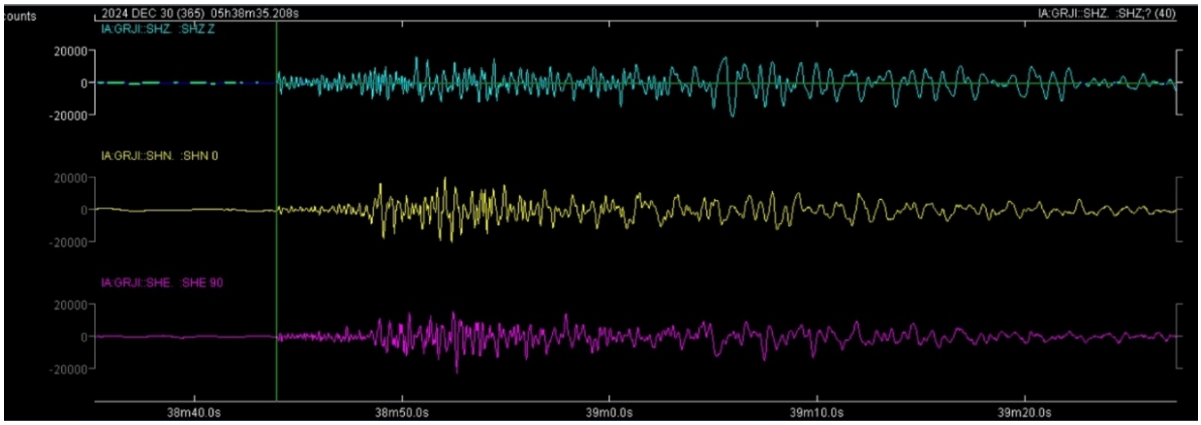

FIGURE 4. Picking the initial impulse of the P wave with SeisGram2K70 software.

This conversion process is required so that the polarity data can be processed quantitatively in focal mechanism software. The acquired polarity data, together with station location information, latitude, longitude, and hypocentral depth, were further processed to determine the geometric parameters of the earthquake source. This process constitutes an essential basis for identifying the nodal planes and fault characteristics that control the earthquake source mechanism under investigation. The determination of these geometric parameters generally includes the strike, dip, and rake values, which represent the orientation and movement direction of the fault plane [27]. The results of the P-wave polarity picking for the Gresik earthquake are presented in TABLE 3.

TABLE 3. Initial P-Wave Motion at the Recording Stations of the Gresik Earthquake.

No	ID Station	Site Sensor	P-Onset
1	BAJI	Bangkalan, Madura	-1 (dilatation)
2	GRJI	Panceng, Gresik	1 (compression)
3	KMMI	Kalianget, Madura	1 (compression)
4	MLJM	Mantup, Lamongan	-1 (dilatation)
5	PCJI	Sudimoro, Pacitan	-1 (dilatation)
6	PPJI	Tretes,Pasuruan	1 (compression)
7	PWJI	Pagerwojo, Tulungagung	-1 (dilatation)
8	SNJI	Sawahan, Nganjuk	1 (compression)
9	SWJI	Geneng, Ngawi	1 (compression)
10	TBJI	Tambak boyo, Tuban	1 (compression)
11	WGJM	Wringinanom, Gresik	-1 (dilatation)
12	BPMJM	Pademawu, Pamekasan	-1 (dilatation)
13	BLJI	Banyuglugur, Situbondo	1 (compression)
14	GGJM	Gabus, Grobogan	-1 (dilatation)
15	LUJI	Lumbang, Pasuruan	-1 (dilatation)
16	BAPJI	Kliyur, Ponorogo	-1 (dilatation)
17	SEJI	Senori, Tuban	-1 (dilatation)
18	SIJM	Sidoarjo	1 (compression)

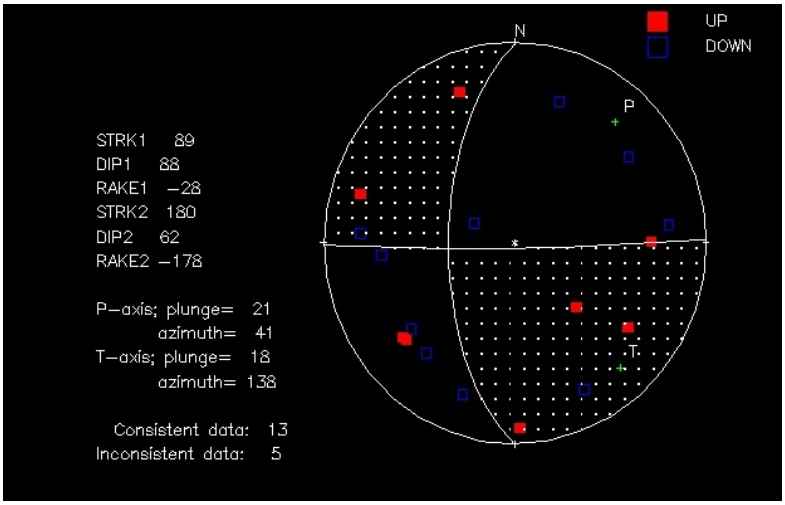

FIGURE 5. Results of Focal Mechanism Analysis of the Gresik Earthquake on December 30, 2024.

Based on the results of data processing using the Seisgram2K, Azmtak, and PINV software, a focal mechanism diagram was obtained, as shown in FIGURE 5. The first nodal plane is characterized by a strike of 89°, a dip of 88°, and a rake of −28°, while the second nodal plane has a strike of 180°, a dip of 62°, and a rake of −178°. Both nodal planes represent two possible fault planes that geometrically satisfy the focal mechanism solution. The earthquake source mechanism analysis based on the focal mechanism solution indicates that the event was dominated by a strike-slip faulting mechanism. This interpretation is supported by the rake values of both nodal planes, which are close to 0° or ±180°, particularly for the second nodal plane with a rake of −178°, indicating an almost pure horizontal displacement (FIGURE 6). A rake value approaching ±180° indicates the dominance of horizontal movement, which is the primary characteristic of a strike-slip fault mechanism [5].

The first nodal plane has a strike orientation of 89° with a dip angle of 88°, indicating an almost vertical fault plane. Meanwhile, the second nodal plane is characterized by a strike of 180° and a dip of 62°, which also reflects strike-slip fault characteristics. A steep to nearly vertical fault plane orientation is a common characteristic of shallow crustal strike-slip faults, reflecting a stress regime in which horizontal stress is more dominant than vertical stress [28].

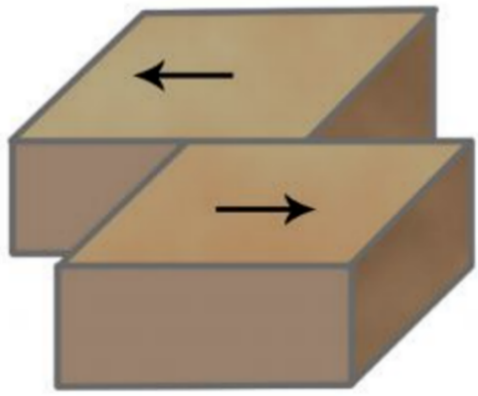

FIGURE 6. Visualization of the Strike-Slip Fault Plane.

The orientation of the principal stress axes further supports the interpretation of a strike-slip faulting mechanism. The maximum compressional axis (P-axis) has a plunge of 21° with an azimuth of 41°, while the maximum tensional axis (T-axis) has a plunge of 18° with an azimuth of 138°. The relatively small plunge values on both axes indicate that the orientation of the principal stresses tends to be horizontal. This condition suggests a predominantly horizontal stress regime, which is commonly found in strike-slip tectonic environments [29].

Based on the Active Fault Map of Indonesia published by PUSGEN (2024), the epicenter of the Gresik earthquake is located along the RMKS–Tuban 3 Fault, which is part of the Rembang–Madura–Kangean–Sakala (RMKS) fault system. This fault system is characterized by a dominant strike-slip mechanism with a general west–east to northwest–southeast orientation and serves as one of the sources of shallow earthquakes in northern East Java. This characteristic is also supported by regional tectonic studies showing that the East Java region is influenced by complex interactions among active fault systems [6, 30].

The source mechanism analysis derived from the focal mechanism solution indicates that the Gresik earthquake was dominated by a strike-slip faulting mechanism with a weak oblique component. This oblique component is indicated by a rake value that does not lie exactly at 0° or ±180°, but still remains within the range dominated by horizontal movement. This mechanism shows strong consistency with the kinematic characteristics of the RMKS–Tuban 3 Fault, suggesting that the earthquake represents an expression of tectonic activity along this fault segment. Although the Gresik region is also influenced regionally by the Kendeng Zone, which is predominantly characterized by thrust faulting as a response to regional compressional forces associated with the subduction of the Indo-Australian Plate south of Java Island [6], In a broader regional context, the East Java region is known to exhibit complex interactions between tectonic deformation and magmatic activity, particularly within the back-arc zone controlled by thrust fault systems and regional compressional structures (Lupia et al., 2022). In addition, crustal deformation on Java Island is also influenced by shallow crustal fault activity that accommodates part of the tectonic deformation [30]. the results of this study demonstrate that tectonic deformation in northern East Java is complex and accommodated by more than one fault system. This condition indicates an interaction between the regional compressional regime and local deformation, resulting in variations in earthquake source mechanisms in the area. In this context, the RMKS Fault acts as a strike-slip fault system that accommodates lateral strain components and serves as a source of local earthquakes with strike-slip mechanisms.

Considering the epicentral location along the RMKS–Tuban 3 Fault, the relatively shallow earthquake depth, and the consistency of the derived source mechanism, the 30 December 2024 Gresik earthquake is interpreted as being caused by activity along the RMKS–Tuban 3 Fault. This interpretation is based on the consistency between the focal mechanism parameters and the regional geological conditions. These findings emphasize that strike-slip fault systems in northern East Java play a significant role as sources of local earthquakes and should be given particular attention in seismic hazard assessments for Gresik Regency and surrounding areas. These results also demonstrate the importance of integrating seismic observation data

and regional geological information to achieve a more comprehensive understanding of earthquake source characteristics.

Earthquake Scenario Modeling

Earthquake scenario modeling in the Gresik region was carried out using the same epicentral parameters as the earthquake that occurred on 30 December 2024. In this scenario, the earthquake magnitude was simulated at M 6.2, referring to the Indonesian Active Fault Map published by PUSGEN (2024), which indicates that the RMKS–Tuban 3 Fault System has the potential to generate earthquakes with a maximum magnitude of up to 6.2. The use of maximum magnitude in scenario modeling is a common approach in seismic hazard analysis to represent the maximum possible ground-shaking conditions that may occur in a region [2, 31].

The scenario modeling of a magnitude 6.2 earthquake is intended to provide a quantitative representation of the spatial distribution of zones potentially subjected to strong ground shaking. This analysis includes the potential increase in shaking intensity (MMI) in densely populated residential areas, industrial zones, and critical infrastructure in Gresik Regency and surrounding regions. Therefore, the results of this modeling are not only academic in nature but also have direct implications for disaster mitigation efforts and risk-based spatial planning. The results of the magnitude 6.2 earthquake scenario modeling are presented in FIGURE 7.

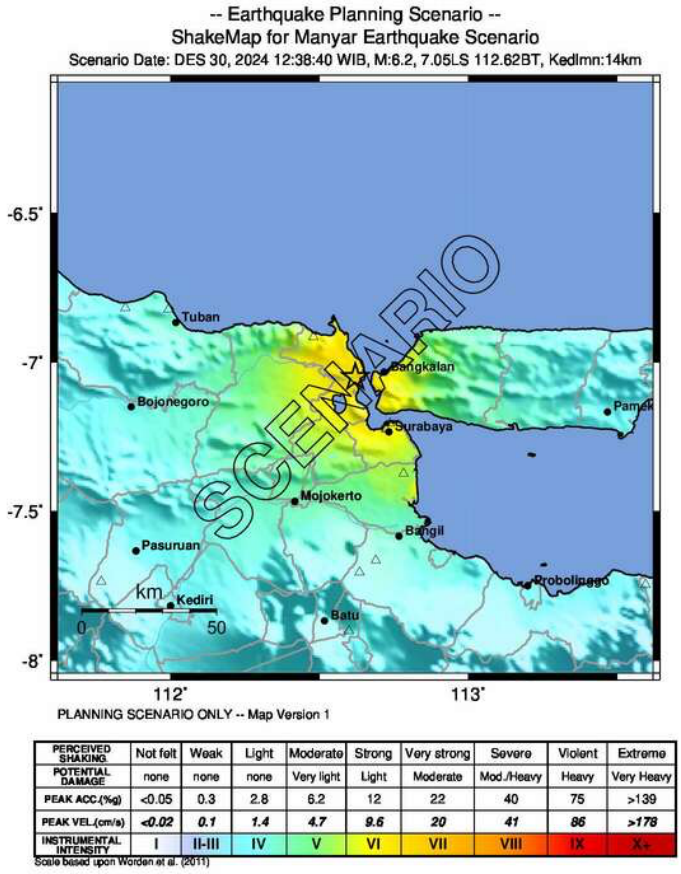

FIGURE 7. Shakemap Scenario of the Gresik Earthquake with Magnitude M 6.2.

FIGURE 7 illustrates the results of the earthquake scenario modeling for Gresik with a magnitude of M 6.2 at a depth of 14 km. The Shakemap displays the spatial distribution of Peak Ground Acceleration (PGA), Peak Ground Velocity (PGV), and instrumental seismic intensity (MMI) across the affected area. These parameters are the primary indicators in evaluating ground-shaking impacts, where PGA and PGV represent ground-motion characteristics, while MMI describes the level of impact perceived by humans and the potential for building damage. [10-11].

Based on the Shakemap scenario for the M 6.2 earthquake, the spatial distribution of shaking intensity exhibits clear variations influenced by the distance from the epicenter, local geological conditions, and seismic wave propagation characteristics. This variation indicates that the distribution of ground shaking is not homogeneous, but rather controlled by a combination of source, path, and local site condition factors. The modeling results indicate that areas surrounding the epicenter, particularly within Gresik Regency, experience maximum shaking intensities of up to VI–VII MMI, as indicated by the dominance of dark yellow colors on the Shakemap. Intensities in the range of VI–VII MMI indicate significant damage potential, which is generally associated with increased shaking levels as represented in the macroseismic intensity scale [11]. This intensity level represents strong shaking felt by nearly all residents, causing many people to become frightened and rush outdoors. At this intensity, heavy furniture may shift, wall plaster may fall, and buildings with poor construction quality or those not designed to be earthquake-resistant are likely to experience light to moderate damage.

As the distance from the epicenter increases, shaking intensity gradually decreases. The City of Surabaya, western parts of Bangkalan Regency, and eastern parts of Lamongan Regency generally experience intensities of around VI MMI, where strong shaking is felt by all residents, some individuals have difficulty standing or walking steadily, heavy furniture may move, and minor damage to non-structural building elements, such as wall cracks and falling plaster, may occur. This decrease in intensity reflects the attenuation process of seismic wave energy due to geometric spreading and energy dissipation during wave propagation, as represented in the Ground Motion Prediction Equation (GMPE) model [32]. Meanwhile, more distant areas such as Tuban, Bojonegoro, Mojokerto, and Pasuruan exhibit lower intensities of approximately IV MMI, characterized by shaking felt by many people inside buildings, especially during daytime, but generally not causing significant structural damage. Nevertheless, local variations may still occur due to the influence of site-specific geological conditions, such as the presence of soft sediments that can amplify ground shaking (site amplification).

The observed pattern of decreasing shaking intensity reflects the attenuation of seismic wave energy with increasing distance from the source, as well as the influence of geological heterogeneity along the propagation path, which contributes to spatial variations in ground shaking levels across the region. Therefore, the results of this modeling confirm that seismic hazard evaluation cannot be based solely on the distance from the earthquake source, but must also take into account local geological conditions and wave propagation characteristics. These findings are consistent with various previous studies showing that the combination of

earthquake source, seismic wave propagation and site condition factors plays an important role in determining the distribution of earthquake ground shaking [10, 14].

CONCLUSIONS

The results of this study indicate that the Gresik earthquake on 30 December 2024 was controlled by a strike-slip faulting mechanism with a weak oblique component. This is evidenced by the focal mechanism modeling results, in which the first nodal plane has a strike of 89°, a dip of 88°, and a rake of −28°, while the second nodal plane exhibits a strike of 180°, a dip of 62°, and a rake of −178°. Rake values close to 0° to ±180°, combined with nearly vertical fault plane orientations, indicate the dominance of horizontal slip in the earthquake source mechanism. A comparison between the orientations of the two nodal planes and the 2024 Indonesian Active Fault Map (PUSGEN) shows that the second nodal plane is more consistent with the orientation and kinematic characteristics of the RMKS–Tuban 3 Fault. Therefore, the second nodal plane is interpreted as the actual fault plane controlling the earthquake event. This consistency strengthens the interpretation that seismic activity in the Gresik area is closely related to the RMKS fault system, which acts as a source of shallow earthquakes in northern East Java. Furthermore, scenario earthquake modeling with a maximum magnitude of M 6.2, simulated based on the maximum potential of the RMKS–Tuban 3 Fault System, indicates that Gresik Regency may experience strong ground shaking with maximum intensities reaching VI–VII MMI. Surrounding areas, including Surabaya City, the eastern part of Lamongan Regency, and the western part of Bangkalan Regency, are expected to experience shaking intensities of up to VI MMI. This intensity distribution indicates that the impact of ground shaking is not limited only to areas near the epicenter, but can also extend to surrounding regions with varying levels of damage.

These findings emphasize that although the 30 December 2024 Gresik earthquake had a relatively small magnitude, the presence and activity of the RMKS–Tuban 3 Fault pose a significant seismic hazard and should be carefully considered in earthquake mitigation efforts in Gresik and its surrounding regions. Thus, the results of this study can serve as a basis for disaster mitigation planning, particularly in improving preparedness and strengthening infrastructure in earthquake-prone areas. However, this study has several limitations. In the ShakeMap and focal mechanism analyses, the results still depend on the availability and distribution of seismic stations, especially due to the relatively small earthquake magnitude, which limits the number of recorded stations and may affect the accuracy of the results. In addition, the scenario modeling approach is still based on Ground Motion Prediction Equations (GMPE) and site condition assumptions, and therefore does not fully represent detailed local geological conditions. For future research, it is recommended to use more detailed geological and geotechnical data, such as direct measurements of Vs30 parameters, as well as to integrate other methods such as microtremor analysis or numerical simulations to improve result accuracy. Furthermore, the development of probabilistic seismic hazard analysis (PSHA) is necessary to obtain a more comprehensive assessment of earthquake risk in the Gresik region and its surroundings.

REFERENCES

[1] P. Bird, "An updated digital model of plate boundaries," *Geochemistry, Geophysics, Geosystems*, vol. 4, no. 3, Mar. 2003, doi: 10.1029/2001GC000252.

[2] M. Irsyam *et al.*, *Peta Sumber dan Bahaya Gempa Indonesia Tahun 2017*. Jakarta: Pusat Studi Gempa Nasional, 2017.

[3] P. Kearey, K. A. Klepeis, and F. J. Vine, *Global tectonics*. John Wiley & Sons, 2009.

[4] H. F. Reid, "The mechanism of the earthquake, the California earthquake of April 18, 1906," *Report of the Research Senatorial Commission, Carnegie Institution, Washington, DC*, vol. 2, pp. 16–18, 1910.

[5] P. M. Shearer, *Introduction to seismology*. Cambridge university press, 2019.

[6] PuSGeN, "Peta Sumber dan Bahaya Gempa Indonesia Tahun 2024," 2024.

[7] A. H. Satyana, E. Erwanto, and C. Prasetyadi, "Rembang–Madura–Kangean–Sakala (RMKS) Fault Zone, East Java Basin: The origin and nature of a geologic border," Bandung, 2004.

[8] BMKG, "Katalog Gempabumi Merusak 1821-2024," Mar. 2025.

[9] S. Bahri and M. Madlazim, "Pemetaan Topografi, Geofisika Dan Geologi Kota Surabaya," *Jurnal Penelitian Fisika dan Aplikasinya (JPFA)*, vol. 2, no. 2, pp. 23–28, 2012.

[10] C. B. Worden, D. J. Wald, T. I. Allen, K. Lin, D. Garcia, and G. Cua, "A revised ground-motion and intensity interpolation scheme for ShakeMap," *Bulletin of the Seismological Society of America*, vol. 100, no. 6, pp. 3083–3096, 2010.

[11] D. J. Wald, V. Quitoriano, T. H. Heaton, and H. Kanamori, "Relationships between peak ground acceleration, peak ground velocity, and modified Mercalli intensity in California," *Earthquake spectra*, vol. 15, no. 3, pp. 557–564, 1999.

[12] C. B. Worden and D. Wald, "ShakeMap Manual," 2024.

[13] J. J. Bommer, P. J. Stafford, and J. E. Alarcón, "Empirical equations for the prediction of the significant, bracketed, and uniform duration of earthquake ground motion," *Bulletin of the Seismological Society of America*, vol. 99, no. 6, pp. 3217–3233, 2009.

[14] J. Douglas, "Earthquake ground motion estimation using strong-motion records: A review of equations for the estimation of peak ground acceleration and response spectra," *Earth. Sci. Rev.*, vol. 61, no. 1–2, pp. 43–104, 2003, doi: 10.1016/S0012-8252(02)00112-5.

[15] V. Cronin, "A draft primer on focal mechanism solutions for geologists," 2004.

[16] A. Lomax, P. Denton, and J.-L. Berenguer, "SeisGram2K-School Users Guide," 2014.

[17] K. N. Suarbawa, I. P. Adnyana, and A. D. Lestari, "Pemetaan Daerah Rawan Gempabumi Berdasarkan Nilai Parameter Kerapuhan Batuan Dan Peak Ground Acceleration(PGA) Di Wilayah Bali," *Kappa Journal*, vol. 8, no. 1, pp. 12–15, Apr. 2024, doi: 10.29408/kpj.v8i1.24283.

[18] E. Prasetyawati Umar, H. Bakri, and M. Karnaen, "Mekanisme Sumber Gempabumi (Focal Mechanism) Manokwari," 2016.

[19] V. A. Harnindra, B. Sunardi, and B. J. Santosa, "Implikasi Sesar Kendeng Terhadap Bahaya Gempa Dan Pemodelan Percepatan Tanah di Permukaan di Wilayah Surabaya," *Jurnal Sains dan Seni ITS*, vol. 6, 2017.

[20] H. Leopatty, R. Efendi, M. N. Rande, I. F. Asyhar, and M. Cholidani, "Identifikasi Tingkat Getaran Gempa di Kabupaten Sigi Berdasarkan Skenario Shakemap Mw 6,9 Sesar Palu Koro," *Gravitasi*, vol. 20, no. 2, pp. 42–46, Dec. 2021, doi: 10.22487/gravitasi.v20i2.15552.

[21] D. M. Boore and G. M. Atkinson, "Ground-Motion Prediction Equations for the Average Horizontal Component of PGA, PGV, and 5%-Damped PSA at Spectral Periods between 0.01 s and 10.0 s," *Earthquake Spectra*, vol. 24, no. 1, pp. 99–138, 2008, doi: 10.1193/1.2830434.

[22] I. Irwandi, Muzli, Muksin, K. Jamaluddin, Zulfakriza, and Joni, "GMPE based Shakemap Generation of Peak Ground Motion and Intensity Maps for Pidie Jaya Earthquake," in *Journal of Physics: Conference Series*, Institute of Physics Publishing, Dec. 2018. doi: 10.1088/1742-6596/1120/1/012092.

[23] R. D. Borcherdt, "Estimates of site-dependent response spectra for design (methodology and justification)," *Earthquake Spectra*, vol. 10, no. 4, pp. 617–653, 1994, doi: 10.1193/1.1585791.

[24] D. M. Boore, "Can site response be predicted?," *Journal of Earthquake Engineering*, vol. 8, no. 1, pp. 1–41, 2004, doi: 10.1142/S1363246904001467.
[25] J. C. Lahr and J. A. Snoke, "Handbook of Earthquake and Engineering Seismology," *Handbook of Earthquake and Engineering Seismology*, 2002.
[26] J. L. Hardebeck and P. M. Shearer, "A new method for determining first-motion focal mechanisms," *Bulletin of the Seismological Society of America*, vol. 92, no. 6, pp. 2264–2276, 2002.
[27] K. Aki and P. Richards, *Quantitative seismology*. MIT Press, 2002.
[28] E. M. Anderson, "The dynamics of faulting and dyke formation with applications to Britain," *(No Title)*, 1951.
[29] M. Lou Zoback, "First-and second-order patterns of stress in the lithosphere: The World Stress Map Project," *J. Geophys. Res. Solid Earth*, vol. 97, no. B8, pp. 11703–11728, 1992.
[30] A. Koulali *et al.*, "The kinematics of crustal deformation in Java from GPS observations: Implications for fault slip partitioning," *Earth Planet. Sci. Lett.*, vol. 458, pp. 69–79, Jan. 2017, doi: 10.1016/j.epsl.2016.10.039.
[31] M. D. Petersen *et al.*, "The 2014 United States National Seismic Hazard Model," *Earthquake Spectra*, vol. 31, no. 1S, pp. S1–S30, Dec. 2015, doi: https://doi.org/10.1193/120814EQS210M.
[32] D. M. Boore, J. P. Stewart, E. Seyhan, and G. M. Atkinson, "NGA-West2 equations for predicting PGA, PGV, and 5% damped PSA for shallow crustal earthquakes," *Earthquake Spectra*, vol. 30, no. 3, pp. 1057–1085, 2014.